International Journal of Thermal Sciences 129 (2018) 426–433

Contents lists available at ScienceDirect

International Journal of Thermal Sciences

journal homepage: www.elsevier.com/locate/ijts

Liquid–vapor phase behavior and operating characteristics of the capillary evaporator of a loop heat pipe at start-up

M. Nishikawara*, K. Otani[1], Y. Ueda, H. Yanada

Toyohashi University of Technology, 1-1, Hibarigaoka, Tenpaku-cho, Toyohashi, Aichi, 441-8580, Japan

ARTICLE INFO

Keywords:
Liquid-vapor interface
Loop heat pipe
Phase displacement
Porous media
Start-up
Visualization

ABSTRACT

The liquid–vapor phase distribution and displacement in the capillary evaporator of a loop heat pipe (LHP) are key phenomena affecting the steady-state and transient operating behavior. This study conducts optical observation of liquid–vapor phase behavior in the evaporator using a transparent glass tube heated by far-infrared radiation during start-up of the LHP. A quartz wick-acetone LHP system is designed, fabricated, and operated successfully with a heat flux of 1 W/cm^2 transported by the cylindrical evaporator. To investigate effect of the liquid–vapor phase distribution in the evaporator at the initial state, start-up experiments with eight phase patterns—which are either liquid-saturated or two-phase in each of the inlet of the vapor line, grooves, and compensation chamber (CC)—are performed. The phase distribution affects the temperature profile although it has no effect upon the steady-state characteristics, and nucleate boiling occurs in the wick or groove simultaneously with evaporator-temperature drop when both the grooves and the inlet of the vapor line are completely filled with liquid. Liquid–vapor displacements from start-up to the steady-state are classified into four transient behaviors, which include boiling in the CC and meniscus oscillation at the three phase contact line within the case, wick, and groove.

1. Introduction

The thermal-control device known as loop heat pipes (LHPs) have recently attracted attention in various fields. LHPs are two-phase loop systems accompanied by a phase change of a working fluid and capillary pressure; thus, it can transport heat in large quantities through the use of latent heat. LHP applications include thermal management of batteries [1], IGBTs of power semiconductor devices [2], and CPU processors for fanless desktop PCs [3].

Previous studies have reported that LHPs show an oscillation or hysteresis of temperature [4–9], so their reliability is insufficiently high. Vershinin et al. presented three types of temperature hysteresis due to heat transfer in the evaporator: a liquid metastable state in the compensation chamber (CC); an initial phase distribution in the LHP; and a temperature oscillation due to a shortage of working fluid [4,5]. Ku et al. demonstrated temperature oscillation with high frequency when the liquid–vapor interface is at the inlet or outlet of the condenser with a high amplitude induced by large thermal mass attached to the evaporator and cooling condition [6,7]. Li et al. reported temperature oscillation at a low heat load with a copper–water LHP [8]. Nishikawara et al. reported temperature oscillation at a low heat load due to boiling in the CC [9]. These transient or quasi-steady phenomena are caused by the behavior of the liquid–vapor interface in the LHP. The interface behavior at start-up is particularly complicated, which causes difficulty of the successful start-up and various start-up scenarios.

Kaya et al. experimentally investigated low-power start-up of the LHP with a nickel wick [10]. The latest start-up was 251 min after the start of heating with a 0.020-W/cm^2 heat flux; the evaporator was located 208 cm vertically above the condenser. It was concluded that the loop orientation affects the start-up time and the required superheat of the evaporator, and that vapor bubbles in the grooves promote early start-up. Huang et al. classified start-up characteristics into four modes of failure, oscillating, overshoot, and normal according to heat load [11]. Wang et al. showed that the lowest heat flux required for start-up of a copper–water LHP was 0.25 W/cm^2, and that LHPs started earlier with thicker wicks under low power [12]. However, the above studies did not control the initial liquid–vapor phase distribution in the evaporator and CC, and ignored any effect this may have.

Maydanik et al. conducted LHP experiments with control of the initial phase distribution by varying the filling ratio of the working fluid R-152A, the orientation in the gravity field, and the cooling temperature [13]. They classified the fluid into the following four phase

* Corresponding author.
E-mail address: nishikawara@me.tut.ac.jp (M. Nishikawara).
[1] Currently at SUZUKI MOTOR CORPORATION, 300 Takatsuka-cho, Minami-ku, Hamamatsu-shi, Shizuoka, 432-8611 Japan.

https://doi.org/10.1016/j.ijthermalsci.2018.03.023
Received 2 October 2017; Received in revised form 5 February 2018; Accepted 23 March 2018

distributions according to the presence or absence of a liquid–vapor interface in the grooves and core of the CC: situation 1 occurs when the liquid–vapor interface appears only in the grooves; situation 2 occurs when the interface appears only in the core; situation 3 occurs when the interface appears in both the groove and the core; and situation 4 occurs when there is no interface in either. The lowest heat flux required for start-up varied from 0.015 to 0.3 W/cm^2 depending on the situation. Ku (1999) also explained the start-up characteristics in detail based on the above classification [14]. Various start-up characteristics are introduced with on-orbit and ground tests as an example [15]. Installation of a start-up heater attached to the CC is emphasized to flood the entire loop with liquid and guarantees a successful start-up. Pressure spikes, pressure surges, temperature drops, and deprime due to cold-liquid injection into the CC are also explained, together with cycles of start-up and shutdown. As described above, the start-up characteristics of the LHP are affected by the initial phase distribution in the evaporator and CC; however, visualization experiments controlling the initial phase distribution have not been performed, nor has the liquid–vapor phase displacement in the evaporator from the initial to the steady-state been investigated.

The evaporators of the LHPs and capillary pumped loops have been visualized by optical [16–21], neutron [22,23], and infrared rays [21,24]. Regions of interest have included the entire loop [22], the cross-section of the evaporator [16,19,21,23,24], the core in the wick [17,20], and the outer surface of a flat-disk-shaped evaporator [18]; visualization of the entire groove and the wick surface applied to heat flux has not been carried out. Thus, more investigation is needed of the start-up characteristics, taking into account the initial phase distribution based on visualization.

Hence, in this study, optical-visualization experiments during LHP operation are performed to study how the initial liquid–vapor distribution affects start-up characteristics. The characteristics at low heat flux are investigated because temperature overshoot (temperature drop) which presents unfavorable characteristics for practical use occurs as previously reported [10,13,15]. An LHP experimental apparatus for visualization of the wick surface and grooves in the cylindrical evaporator is designed based on the LHP steady-state-analysis model and fabricated with a transparent glass tube as the evaporator case and the non-contact radiation heating system, as shown in Fig. 1. The effects of the phase distribution in the inlet of the vapor line (VL), grooves and CC on the start-up behavior and phase displacement scenarios are reported.

2. Loop-heat-pipe experimental visualization apparatus

In order to visualize phase-change phenomena at high heat flux in the evaporator, an LHP is designed for a maximum heat flux of 20 W/cm^2. The LHP steady-state analysis model is developed based on the model in Ref. [25], where the temperature and pressure are calculated by energy conservation equations and the pressure loss in each component.

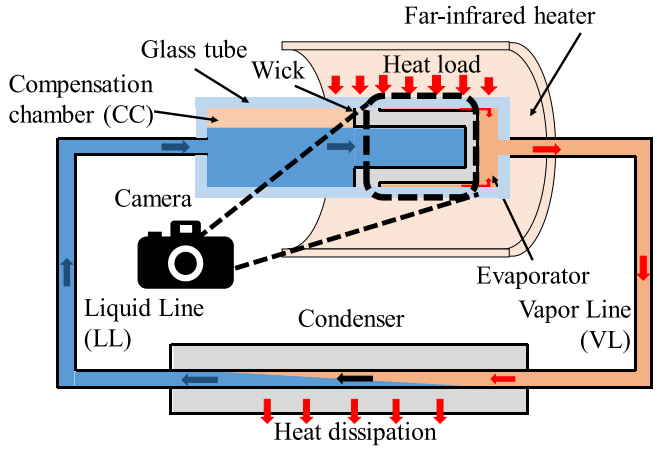

Fig. 1. Schematic of the LHP experimental apparatus for visualization.

The capillary limit occurs when the total pressure loss of an LHP, ΔP_{all}—including pressure loss in the VL, condenser, liquid line (LL), and wick—exceeds the maximum capillary force of the wick, P_{cap_max}. The transported heat amount at the capillary limit is defined as the maximum transported heat, $\dot{Q}_{\max}$,

$$P_{cap.\max} = \Delta P_{all}(\dot{Q}_{\max}). \quad (1)$$

The model assumes that $\dot{Q}_{\max}$ is applied only to the surface of the evaporator case and radiation heat transfer from the heaters into the evaporator is ignored. A parametric analysis based on the diameters and lengths of the evaporator and transport lines (VL, LL, and condenser) and the pore radius of the wick was conducted. The capillary limit was found to be largely dominated by the pore radius of the wick and the inner diameters of the VL and condenser in this LHP. The LHP was designed from the analytical results under the constraints of the experimental environment. Table 1 lists the main characteristics. Acetone was selected as the working fluid. The maximum transported heat of the designed LHP is 400 W (20 W/cm^2).

To visualize the evaporator during LHP operation, a quartz glass tube is used for the evaporator case and the evaporator is heated with far-infrared ceramic heaters, as shown in Fig. 2. The wavelength range of the heater is 3.75–6.1 μm, and the emissivity of the quartz glass is 0.6 in the range [26], so non-contact heating by radiation is possible with this configuration. The CC is integrated into the quartz tube connected to the stainless-steel tubes of the VL and LL.

The wick installed in the quartz tube is cylindrical in shape with one side closed, and it has been machined with ten rectangular grooves of 2-mm width and 1-mm depth on the outer side. The groove length is 45 mm so as to make a seal part of 5-mm length between the wick and case and to prevent vapor from flowing to the CC through the clearance. Liquid accumulated in the CC is supplied to the wick from the wick core of 47.5-mm length.

A quartz sintered material with particles ranging in size from a few μm to a dozen μm is used as the porous medium for the wick. Fig. 3 shows a SEM picture of the wick surface and a reconstructed rendering by nano-X-ray computed tomography. The micropores found in Fig. 3 play a role in the emergence of capillary pressure. The pore radius distribution measured by the mercury intrusion technique is shown in Fig. 4; the peak radius is 3.2 μm and the porosity is 37%.

The developed evaporator is shown in Fig. 2b. After the wick was installed in the case, the sealing ability between the case and the wick was verified by a bubble-point test [27]. Firstly, the wick core and CC were filled with the working liquid; then, nitrogen gas was pressed from the VL side. When the pressure increases, the gas penetrates the wick and gas bubbles are observed in the CC at a certain pressure. This is known as the bubble-point pressure, P_b, and the maximum pump pressure of the evaporator. The bubble-point pressure measured with the developed evaporator is 10.5 kPa. From the result, the curvature radius, r_b, of the liquid–vapor interface at the bubble point is calculated with Young-Laplace equation,

$$r_b = \frac{2\sigma}{P_b}\cos\theta, \quad (2)$$

Table 1
LHP characteristics.

Component	Length (mm)	Outer diameter (mm)	Inner diameter (mm)
Wick	50	12.6	7
Evaporator	50	15	12.6
CC	300	15	12.6
Vapor line	436	6.4	4.4
Condenser	950	6.4	4.4
Liquid line	512	6.4	4.4